EUROPEAN JOURNAL OF PURE AND APPLIED MATHEMATICS
2025, Vol. 18, Issue 3, Article Number 6371
ISSN 1307-5543 – ejpam.com
Published by New York Business Global

Effects of Volume Fraction and Chemical Reaction on Inclined MHD Two-Phase Biorheological Flow in a Porous Tumor Region: Heat and Mass Transfer with Soret Effect

Devendra Kumar[1,*], Mahesh Garvandha[1], Sanjeev Kumar[2], Narendra Deo[3]

[1] *Department of Computer and Information Science, University of Technology and Applied Sciences, Shinas, Oman*
[2] *Dr. Bhimrao Ambedkar University, Agra, Uttar Pradesh, India*
[3] *Oncology Unit, Synergy Hospital, Agra, Uttar Pradesh, India*

Abstract. Blood transport has many crucial answers and unanswered questions responsible for the formation of metastasis, growth, and effective treatments. In any therapy (radiotherapy, chemotherapy, or immunotherapy), blood carries the required agents, such as oxygen or pharmacological agents. Blood viscosity and concentration are important factors to study. Two-phase biorheology of the blood is considered with chemical reaction and volume fraction. Heat and mass transport are proposed to study with the Soret application. The angle of inclination of the applied magnetic field is $(0 < \alpha < \pi/2)$. The concentrated agents (drugs) carried by the blood create chemical reactions in the surrounding medium. Thus, the mathematical model is governed by partial differential equations (PDEs) for fluid transport, heat transport, and mass transport. These equations are solved using the mathematical function PDEPE in the software MATLAB. These transport interactions in tumor regions are obtained for fluid velocity, suspension velocity, thermal profiles, and concentration profiles for parameters like Soret number (Sr), volume fraction (ϕ), magnetic intensity (M), Chemical reaction parameter (ϑ), thermal radiation parameter (Rd), etc. These results are validated through graphs and tables obtained. Soret effects vary $(0.5 < Sr < 1.5)$ that reduces transport velocity that will support drug delivery systems. Thermal parameters on blood flow, heat stress, and concentration that help in tumor treatments are described using numerical outputs and depicted through graphs.

2020 Mathematics Subject Classifications: 35Q35, 92C35, 76T20, 76V05, 76S05

Key Words and Phrases: Two-Phase Biorheology, Chemical Reaction, Volume Fraction, Heat and Mass Transport, Soret Application

*Corresponding author.
DOI: https://doi.org/10.29020/nybg.ejpam.v18i3.6371

Email addresses: devendra.kumar@utas.edu.om (D. Kumar), mahesh.garvandha@utas.edu.om (M. Garvandha), sanjeevibs@yahoo.co.in (S. Kumar), deo_narendra@yahoo.co.in (N. Deo)

1. Introduction

Cancer deaths are reported to be the second highest throughout the world after cardiovascular diseases. One out of five deaths is due to cancer. The world has a strong medical infrastructure, and research collaborations are made; even then, this load needs attention, as the WHO report [1] suggests. Generally, tumors are not detected timely, which leads to a significant cause of death. Physiological situations of the tumors are observed in that they are fed by the surrounding blood vessels. Multiphase fluid transport system takes place with volume fraction. The volume fraction is the space occupied by each phase, and the laws of conservation of mass and momentum are satisfied by each phase individually. Baxter & Jain [2–4] investigated the fluid flow in tumors under the effects of pressure and convection. The authors measured the fluid velocity and outward and inward concentration profiles. This investigation experimentally verified that pressure plays an important role in pushing the macromolecules in the tumor region. Diffusion effects are seen in this investigation. Individual blood vessels are ignored, and some of the blood vessels may be leaky due to high blood pressure. Local accumulation of macromolecules is also observed.

In the critical review of Jain [5], fluid(blood) transport plays a key role in growth, metastasis, identification, and survival from tumor deceases. Radiotherapy requires a rich amount of oxygen in the tumor environment, while chemotherapy and immune therapy require a significant amount of drugs that can be carried out through blood vessels, along with blood only. Thus, this study of blood transport with drug suspensions with different parameters becomes a necessity.

In the process of medications, drugs are mixed with a mixture of solid and liquid and transported through the blood throughout the human body. Thus, a study of multiphase fluid flow systems is required, which has been contributed by several researchers. Singh and Singh [6] investigated the transport of fluid-particle suspension along a rectangular channel with volume fraction and a magnetized field applied normally. In this study, the authors introduced that a part of the suspension and fluid make making the one.

Byrne & King [7] studied two-phase solid tumor growth using cells and water in the tumor as two different phases and represented by using mass balance equations. The reaction-diffusion equation was used to understand the tumor growth. Bogdanov et al. [8] provided insight into the situation of the fluid flowing through a medium having pores. Many industrial, biological, fuel extraction, and mining processes are examples of porous flow. Prakash et al. [9] obtained the results for the blood transport through the branched artery having a feverish physiological condition. Normal and axial velocity was evaluated to understand the biofluid transport in the human body. Chaudhary et al. [10], Abbas et al. [11], and Madhura & Shweta [12] studied the fluid transport systems having different suspensions. In medication, fluids are given with strategic drug deliveries considered as multiphase flows with volume fractions. Volume fractions play a vital role when fluid flows through porous media. There are pores in a medium that absorb the suspension-like drug, which is carried by blood in case of flow through the tumor spheroids. That enhances the size of the tumor.

Eldesoky [13] provided a physiological fluid (blood) flow model through a rectangular

channel. The author mainly studied external heat source impacts on the rheology of blood, where a transverse magnetic field is also applicable. In the observation, significant changes are observed in blood flow transport.

Chen et al. [14] used positron emission tomography to understand tumor permeability and blood flow transactions. Thulborn et al. [15] studied the view of chemoradiation, the number of drugs used during chemotherapy, tumor cell volume, and the amount of cell killing volume. Thus, further studies of volume fraction along with heat stress create significant scope in tumor studies.

Vazifehshenas & Bahadori [16] examined drug delivery aspects in the presence of Soret effects to break physiological and biological barriers. Here, mainly, authors have stressed studying fluid(blood) transport, mass transport, and heat transport in the tumor region. It is noted here that increasing the Soret number decreases the tumor temperature, which increases the efficacy of drug delivery.

Wirthl et al. [17], Bera et al. [18] investigated the changes in tumor physiology under multiphase systems of fluid flow-carrying nanoparticles for treatment strategies. The authors studied the changes under the effects of thermal and magnetic conditions. Omamoke et al. [19] investigated blood transport with thermal radiation along with a magnetic field at some inclination in the presence of a heat source. Their application was impacting in treating the tumor diseases and clinical maintenance of high blood pressure by observing decided parameters. Kumar et al. [20] studied blood flowing through the apex of a bifurcated artery having a carotid body tumor. The amount of drug is applied that creates chemical reactions, and this supports tumor treatments by monitoring and measuring the flow rates. An external heat source is applied where an inclined magnetic field is applied to the flow system, which provides significant help to the study.

Liu et al. [21] did a review of common practices in the field of cancer treatment. Fluid transport systems under drug delivery systems supply the antitumor drugs, like personalized nanomaterials. The most common treatment is the spreading of chemicals throughout the whole body through the blood vessels. Thus, the study of blood transport in tumor-surrounding regions with loaded drugs with different parameters is a recent requirement.

Darvishi et al. [22] provided a cost-effective drug delivery system for tumor treatments using magnetized nanoparticles that involves nothing but monitoring of drugs as a model of volume fraction in the presence of heat and mass transfer. Most recently Wang et al. [23] investigated the impacts of porosity and volume fraction to understand the atomic behavior of cancer cells. The authors have used the molecular dynamics method in the formation of hematogenous metastasis. This study has the scope to review heat and mass transfer effects to understand the structures. Shah et al. [24] investigated thermal transport in physiological situations. Thermal shock is introduced in biological systems. The significant and fast change in temperature in biological systems (middle of tissues) is examined using Laplace transforms. Shakya [25] worked on the role of chemistry in tumor development, monitoring, controlling, and treating. The authors examined the chemical reaction of homogeneous and heterogeneous types that change the efficacy of drug delivery systems. Thus, chemical reactions in flow interactions must be focused on

understanding the variations with other parameters. Yadav et al. [26] have conducted an investigation of a two-phase blood flow study through the porous channel. Girema et al. [27] investigated blood transport phenomena in bifurcated arteries where an external heat source is provided. Here authors have used the Soret effect with a transverse magnetic field. The authors found the significant role of Soret number in blood velocity, which gives insight into cardiovascular diseases.

The research gap generated here is that the flowing free fluid surrounding the tumor spheroid interacts with the tumor surface and the pores of the free surface. The flowing fluid carries magnetized drug particles, which are absorbed by pores and enhance the tumor volume. The drugs provided with the blood generate chemical reactions between fluid species, drug particles, and available agents. The present investigation is done for the two-phase biorheology of fluid in the bloodstream surrounding the tumor region. Concentration effects, thermal radiation effects, chemical reaction effects, and Soret effects are examined for fluid velocity and drug particle velocity under various monitored forces. Using the computational approach, the drag force (skin friction on walls), heat transfer rate (Nusselt number), and Sherwood number (mass transfer coefficient) are also obtained.

2. Mathematical Formulation

The flow channel is considered a conducting parallel plate channel at $2b$ apart. The flowing fluid blood of density ρ is considered Newtonian, homogeneous, and viscous. The flowing channel has a rectangular tumor region with pores surrounding it. The non-conducting drug mixture is loaded along with the blood. The flowing region is under an external magnetic field B_0 applied at an inclination of angle α. Mostly, these tumors are found at the bifurcation segment of the arterial flow (channel), where the angle of bifurcation is adjusted to zero. The magnetic field produced due to induction is negligible, and the Reynolds number Re is kept low to maintain the flow laminar. This bifurcation of a large artery into two segments of half flow region was earlier investigated by Zamir & Rouch [28]. Two-dimensional flow is considered to simplify the complex geometry.

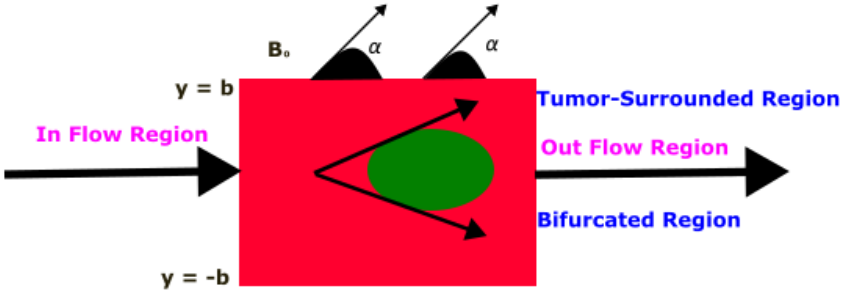

Figure 1: Schematic diagram of the flowing fluid surrounding the tumor spheroid appearing at the apex of the bifurcation.

Assumptions in dimensional equations:

u^*: Blood (fluid) velocity, v^*: suspension (drug) velocity, ρ : fluid density, η: fluid viscosity, p^*: pressure. K_T: thermal conductivity, C_p: specific heat at constant pressure, Q: amount of heat, T: temperature, β : volumetric expansion parameter, β' : volumetric expansion parameter for concentration, θ is the temperature distribution, α : angle of inclination of the applied magnetic field, K^* : porosity parameter, Sr^* : Soret number, D is diffusion.

Where, S (heat source parameter) $= \frac{Qb^2}{K_T}$, P_r(Prandtl number) $= \frac{\rho C_p}{K_T}$, Sc (Schmidt number)$=\frac{\eta}{D\rho}$, M^2 (Magnetic Field Parameter)$=\frac{k\eta}{\sigma b^2}$, ϑ(Chemical Reaction parameter)$=\frac{k_1 b^2 \rho}{\eta}$, Rd (Thermal radiation parameter) $= \frac{16\delta' {T_0}^2}{3k'\tau}$, K(Porosity parameter) $= \frac{k\eta}{\sigma b^2}$, G(Particle mass parameter)$=\frac{m_p \mu}{\rho h^2}$, R(Particle concentration parameter)$=\frac{K' N h^2}{\mu}$.

3. Governing Equations and Illustrations

The flow is under concentration, externally applied heat source under Soret effects, and various physiological situations. The flowing blood carrying some amount of drug is governed by the following mathematical equations.

$$\begin{aligned}(1-\phi^*)\frac{\partial u^*}{\partial t^*} &= (1-\phi^*)(-\frac{1}{\rho}\frac{\partial p^*}{\partial x^*}+\frac{\eta}{\rho}\frac{\partial^2 u^*}{\partial {y^*}^2})+g\beta(T-T_\infty)^*+g\beta'(C-C_\infty)^* \\ &\quad +K^{'}N(u^*-v^*)-\frac{\sigma B_0^2 sin^2\alpha}{\rho}u^*-\frac{1}{K^*}u^*, \qquad (1)\end{aligned}$$

$$m_{_p}\frac{\partial v^*}{\partial t^*}=K^{'}(u^*-v^*), \qquad (2)$$

The flow region gets heated due to the reactions of the drugs provided with the fluid. Moreover, many times external load in physiological situations like inflammations makes the body feverish, and radiations take place that are governed by the energy equation.

$$\frac{\partial T^*}{\partial t^*}=\frac{K_T}{\rho C_p}\frac{\partial^2 T^*}{\partial {y^*}^2}+\frac{Q}{\rho C_p}(T-T_\infty)^*-\frac{\partial q^*}{\partial y^*}. \qquad (3)$$

Chemical reactions and adding the monitored drug concentrate the flowing fluid (blood), and diffusion happens, which is modelled as the concentration-diffusion equation.

$$\frac{\partial C^*}{\partial t^*}=D\frac{\partial^2 C^*}{\partial {y^*}^2}-k_1(C-C_\infty)^*+S_r^*\frac{\partial^2 T^*}{\partial {y^*}^2}. \qquad (4)$$

The non-dimensional for illustrations,

$$x=\frac{x^*}{b}, \quad y=\frac{y^*}{b}, \quad u=\frac{u^*}{\frac{m}{2b\rho}}, \quad v=\frac{v^*}{\frac{m}{2b\rho}}, \quad h=\left(\frac{\frac{-dp^*}{dx^*}}{\frac{\eta m}{2b^3\rho}}\right), \quad K=\frac{K^*}{\frac{b^2\rho}{\eta}},$$

$$\tau=\frac{\eta}{\rho}, \quad t=\frac{t^*}{\frac{b^2\rho}{\eta}}, \quad \theta=\frac{\theta^*}{\frac{m\eta}{2b^3\rho^2}}, \quad C=\frac{C^*}{\frac{m\eta}{2b^3\rho^2}}, \quad Sr=\frac{S_r^*}{D}.$$

Reduced dimensional equations are:

$$\frac{\partial u}{\partial t} = h + \frac{\partial^2 T}{\partial y^2} + \frac{1}{(1-\phi)}(g\beta\theta + g\beta' C - M^2 sin^2\alpha u - R(u-v) - \frac{u}{K}), \tag{5}$$

$$G\frac{\partial v}{\partial t} = u - v, \tag{6}$$

$$\frac{\partial \theta}{\partial t} = (\frac{1}{\tau Pr} + Rd)\frac{\partial^2 \theta}{\partial y^2} + \frac{S}{\tau Pr}\theta, \tag{7}$$

$$\frac{\partial C}{\partial t} = \frac{1}{Sc}\frac{\partial^2 C}{\partial y^2} - \vartheta C + \frac{Sr}{Sc}\frac{\partial^2 \theta}{\partial y^2}, \tag{8}$$

The boundary conditions are:

$$\begin{aligned} u &= e^{-\lambda^2 t}, \quad v = e^{-\lambda^2 t}, \quad \theta = e^{-\lambda^2 t}, \quad C = e^{-\lambda^2 t} \quad \text{at} \quad y = -1, \\ u &\to 0, \quad v \to 0, \quad \theta \to 0 \quad , C \to 0 \quad \text{at} \quad y = 1. \end{aligned} \tag{9}$$

The governing PDEs are solved by the function PDEPE in MATLAB. Figure 2 is the complete flowchart of the process of the PDEPE solver used in solving the governing equations. This is an easy and practical tool for simulating and visualizing models, serving as an alternative approach for solving initial boundary value problems (IBVP) related to parabolic and hyperbolic equations. The PDEPE is a built-in function that employs a second-order spatial discretization technique, which is developed by utilizing x Mesh and t Span parameters. The accuracy, consistency, and expense of the computational approach rely on the mesh size employed. The function PDEPE operates in tandem with the stiff ODE solver ode15 for effective calculations, utilizing time step values that are dynamically modified to maintain the precision of the PDE solutions. The flow is streamlined under consideration of a low Reynolds number. The boundaries considered are closed, and the flow is stable.

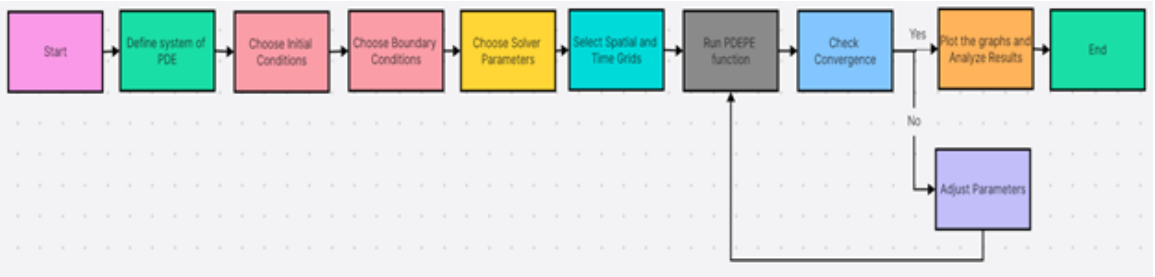

Figure 2: Schematic flow chart of the PDEPE solver.

4. Results and Discussion

The fluid (blood) transport is investigated in the presence of various parameters. The fluid is loaded with a suspension (drug) with different physiological situations, like when an external heat source is applied, the flow region is magnetized at an angle, and the chemical reaction takes place in the tumor's surrounding region. The transport of the fluid and suspension varies and is noted in Figures 3 to 25. Some of the parameters with computable results are fixed and taken as $t = 1, h = 0.5, \beta = 1.5, \beta' = 0.5, K = 2, R = 0.5$(concentration), $G = 0.8$(particle mass), $Pr = 7, S = 0.5, \lambda = 1, M = 0.5, \alpha = \pi/6, \phi = 0.2, Rd = 1$.

Figures 3, 4, 5, and 6 are plotted for varying magnetic field intensity $M(0.5, 1, 1.5)$, porosity parameter $K(2, 3, 4)$, inclination angle $\alpha(\pi/6, \pi/4, \pi/3)$, and volumetric expansion β (1, 1.2, 1.4) at $t = 1$ between $y = -1$ to $y = 1$. Velocity at the walls is almost the same for both phases and rises high in the central part of the flow region. Thus, more drug particles attack the central part of the flow region. The velocity profiles are found to be reduced for higher intensity of magnetic field and increasing angle of inclination. Porosity and volumetric expansion constant are increasing the velocity. The suspension phase is showing less velocity compared to the suspension career velocity.

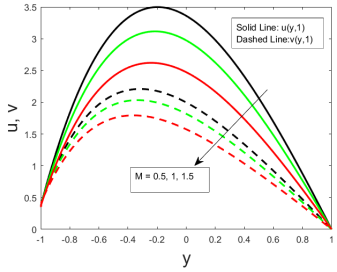

Figure 3: Fluid and suspension velocity for magnetic field intensity M

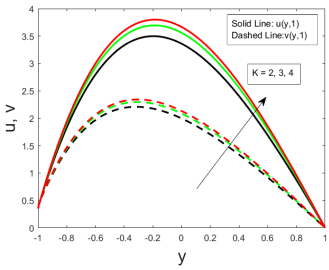

Figure 4: Fluid and suspension velocity for porosity parameter K

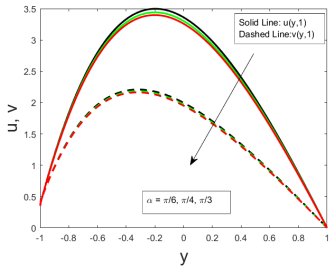

Figure 5: Fluid and suspension velocity for the angle of inclination α

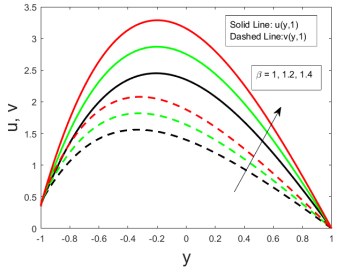

Figure 6: Fluid and suspension velocity for volumetric expansion β.

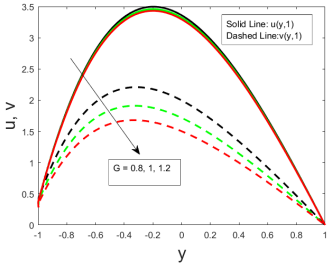

Figure 7: Fluid and suspension velocity for particle mass parameter G.

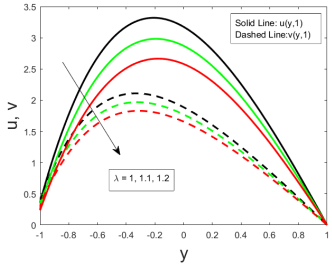

Figure 8: Fluid and suspension velocity for decay parameter λ

Figures 7, 8, 9, and 10 are depicted for particle mass parameter $G(0.8, 1, 1.2)$, decay parameter λ (1, 1.1, 1.2), particle concentration parameter R (0.5, 1, 1.5), volume fraction $\phi(0.02, 0.1, 0.3)$ respectively at $t = 1$ and the flow region is between $y = -1$ to $y = 1$. The

parameter creates a fraction between the free-flowing fluid, suspension, and the pores in the boundaries of the region, thus, velocities represent a significant change in the phase velocities. The only parameter for volume fraction is increasing the velocity of the blood while decay, concentration, and mass parameters reduce the velocity.

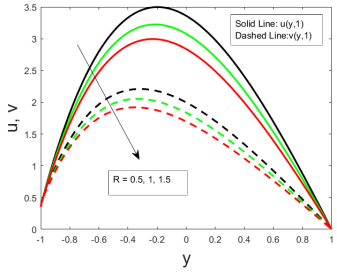

Figure 9: Fluid and suspension velocity for particle concentration R.

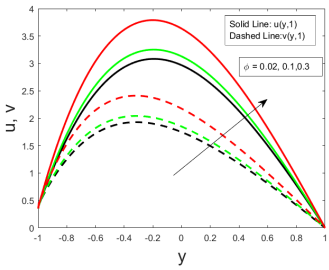

Figure 10: Fluid and suspension velocity for volume fraction ϕ.

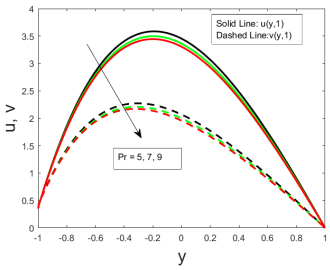

Figure 11: Fluid and suspension velocity for Prandtl number Pr

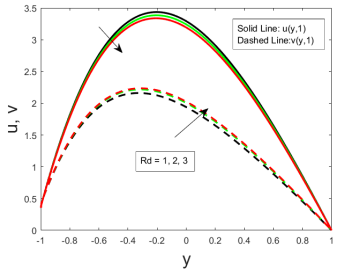

Figure 12: Fluid and suspension velocity for for thermal radiation Rd.

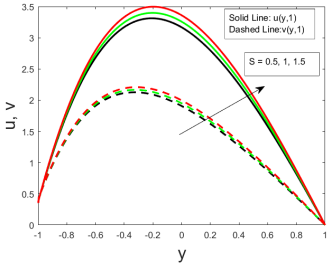

Figure 13: Fluid and suspension velocity for heat source S

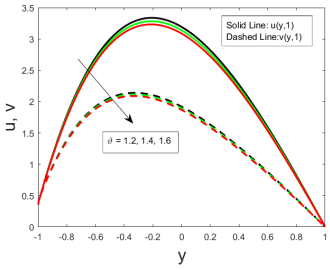

Figure 14: Fluid and suspension velocity for chemical reaction parameter ϑ.

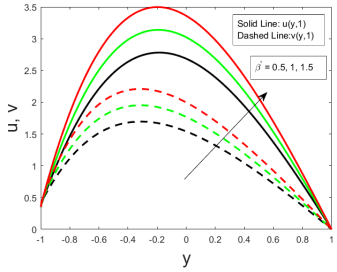

Figure 15: Fluid and suspension velocity for concentration parameter β'.

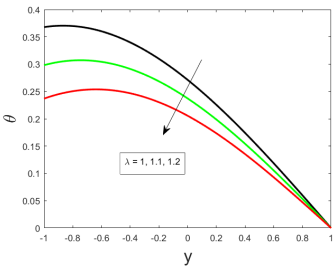

Figure 16: Thermal profile to decay parameter λ.

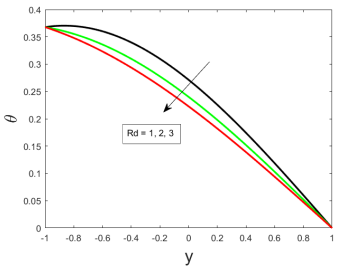

Figure 17: Thermal profile to radiation parameter Rd.

Figure 11 is plotted for varying Prandtl numbers Pr (7, 8, 9), and Figure 12 is depicted for thermal radiation parameter Rd (1, 2, 3) for $t = 1$ and the flowing region between $y = -1$ to $y = 1$. Flows at the boundary are almost zero and higher in the middle of the channel. Both parameters are related to phase turbulence and thermal transport. Thermal transport in the presence of radiation gives a reverse nature of flow in both

phases. The suspension (drug amount) moves fast towards the pores of the tumor's outer surface as pressure is also acting on the walls, while it is kept constant here. Figure 13 is plotted for varying heat sources applied externally, S (0.5, 1, 1.5), in the same geometry that reduces the fluid viscosity, and the internal energy of the flow region increases, so suspension particles move fast, hence enhancing the velocity profiles. Figure 14 is plotted to investigate the variations in flow rates of both phases against the chemical reaction parameter ϑ (1.2, 1.4, 1.6). Both phases reduce the transport rate. Figure 15 is plotted for volumetric expansion of the concentration β' (0.5, 1.0, 1.5), enhancing the velocity as the free space in the flow region increases.

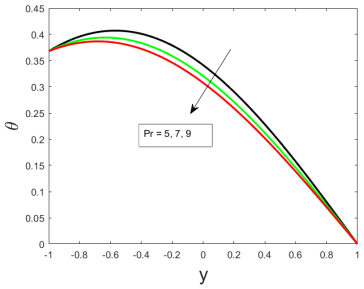

Figure 18: Thermal profile to Prandtl number Pr

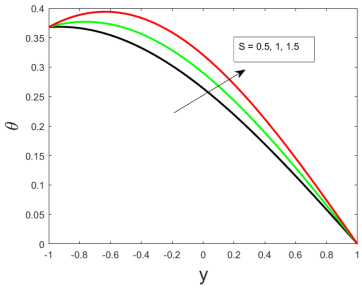

Figure 19: Thermal profile to heat-Source S.

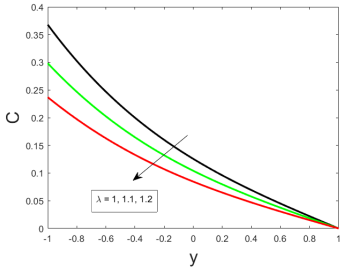

Figure 20: Concentration profile to decay parameter.

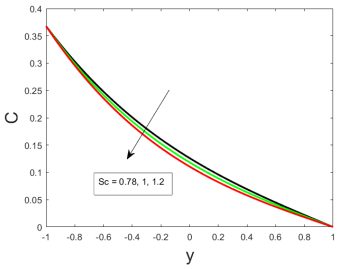

Figure 21: Concentration profile to Schmidt number Sc

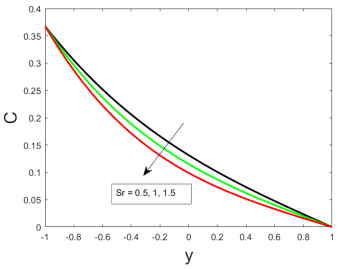

Figure 22: Concentration profile for Soret number Sr

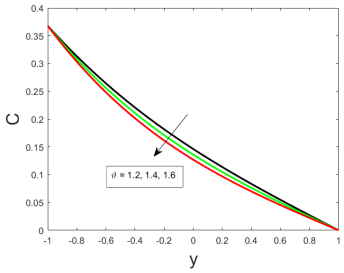

Figure 23: Concentration profile to chemical reaction parameter ϑ

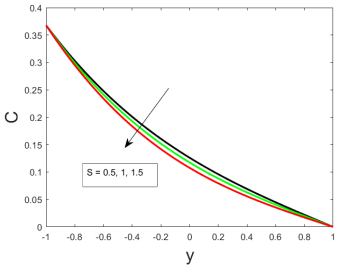

Figure 24: Concentration profile to heat source

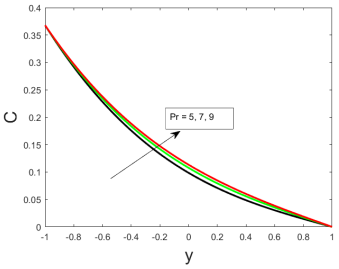

Figure 25: Concentration profile for Prandtl number

Figures 16 to 19 are depicted to examine the variations in thermal profiles. The fixed values considered for different parameters used to obtain the numerical results are $t = 1, Pr = 5, S = 0.5, \lambda = 1, Rd = 1$. Figures 16, 17, and 18 are plotted for decay parameters for varying (1, 1.1, 1.2), thermal radiation parameter Rd (1, 2, 3), and Prandtl number Pr(5, 7, 9), respectively, between the flow region $y = -1$ to $y = 1$. All three are showing that the temperature field is reducing. This is observed that the lower wall $y = -1$ has more thermal impact, while the upper wall $y = 1$ has zero temperature as the applied external heat source is monitored below the channel. Figure 19 is drawn for increasing heat source parameter S (0.5, 1, 1.5) raises the thermal field in the flow region as heat is externally provided, also the homogeneous chemical reaction increases the temperature of the system. This significant change in thermal profiles is treated in strategic thermal and radiation therapies clinically. In drug delivery systems, diffusion is governed by both heterogeneous and homogeneous chemical reactions. In the present investigation, only homogeneous chemical reactions of first order are considered.

Figures 20 to 25 are depicted to show the changes in concentration profiles. The fixed values considered for different parameters used to obtain the numerical results are $t = 1, Pr = 5, S = 0.5, \lambda = 1, Sc = 0.78, Sr = 0.5, \vartheta = 1.2$.

Figures 20, 21, 22, 23, and 24 are plotted for the decay parameter. λ (1, 1.1, 1.2), Schmidt number Sc (0.78, 1, 1.2), Soret number Sr (0.5, 1, 1.5), chemical reaction parameter ϑ (1.2, 1.4, 1.6), and heat source parameter S (0.5, 1, 1.5) respectively, between the flow region $y = -1$ to $y = 1$. All the increasing values reduce the concentration of the tumor-surrounded flow field. This is observed that the lower wall. $y = -1$ has more thermal impact, while the upper wall $y = 1$ has zero temperature as the applied external heat source is monitored below the channel.

Figure 25 is plotted for increasing Prandtl number Pr (5, 7, 9) that raises the concentration of the flow region as heat is externally provided, also the homogeneous chemical reaction increases the energy of the internal system. In such an environment monitored and strategic drug delivery system is improved.

In this investigation, the drug is loaded in the flowing carrier (blood) that creates a drag force on walls, such as Zamir & Roach [28] apart from this, in drug-loaded therapies, thermal transport and mass flow rates are of concern medically. Thus, the drag force (skin friction C_f) appeared on the vessel wall, heat transfer rate (Nusselt number Nu), and rate of mass transfer (Sherwood number Sh) are calculated numerically and listed in Table 1.

$$-C_{f1} = \frac{\partial u}{\partial y} \text{ at } y = -1, \; -Nu1 = \frac{\partial \theta}{\partial y} \text{ at } y = -1, \; -Sh1 = \frac{\partial C}{\partial y} \text{ at } y = -1,$$

$$-C_{f2} = \frac{\partial u}{\partial y} \text{ at } y = 1, \; -Nu2 = \frac{\partial \theta}{\partial y} \text{ at } y = 1, \; -Sh2 = \frac{\partial C}{\partial y} \text{ at } y = 1 \; .$$

Table 1: Values of Skin friction, Nusselt, and Sherwood number at $y = -1$ and $y = 1$

M	λ	ϕ	Pr	Sr	Sc	Rd	S	$-C_{f1}$	$-Nu1$	$-Sh1$	$-C_{f2}$	$-Nu2$	$-Sh2$
0.5								8.3452	0.0177	−0.3502	−4.1584	−0.2923	−0.1096
1	1	0.2	7	0.5	0.78	1.2	0.5	7.6315	0.0177	−0.3502	−3.6372	−0.2923	−0.1096
1.5								6.6759	0.0177	−0.3502	−2.9720	−0.2923	−0.1096
	1							8.6666	0.1423	−0.3967	−4.4495	−0.3721	−0.0849
0.5	1.1	0.2	7	0.5	0.78	1.2	0.5	7.6183	0.1585	−0.3134	−4.0805	−0.3310	−0.0687
	1.2							6.6453	0.1671	−0.2426	−3.7233	−0.2919	−0.0539
		0.02						7.4051	0.1423	−0.3967	−3.9657	−0.3721	−0.0849
0.5	1.1	0.1	7	0.5	0.78	1.2	0.5	7.9135	0.1423	−0.3967	−4.1649	−0.3721	−0.0849
		0.2						8.6666	0.1423	−0.3967	−4.4495	−0.3721	−0.0849
			7					8.6666	0.1423	−0.3967	−4.4495	−0.3721	−0.0849
0.5	1.1	0.2	8	1	0.78	1.2	0.5	8.6163	0.1289	−0.3907	−4.4011	−0.3614	−0.0895
			9					8.5768	0.1180	−0.3858	−4.3631	−0.3527	−0.0933
				0.5				8.6666	0.1423	−0.3967	−4.4495	−0.3721	−0.0849
0.5	1.1	0.2	7	1	0.78	1.2	0.5	8.4770	0.1423	−0.5144	−4.3417	−0.3721	−0.0344
				1.5				8.2880	0.1423	−0.6321	−4.2347	−0.3721	−0.0160
					0.78			8.6666	0.1423	−0.3967	−4.4495	−0.3721	−0.0849
0.5	1.1	0.2	7	0.5	1	1.2	0.5	8.5293	0.1423	−0.4159	−4.3282	−0.3721	−0.0779
					1.2			8.4118	0.1423	−0.4348	−4.2254	−0.3721	−0.0700
						1		8.7176	0.1813	−0.4077	−4.4877	−0.3920	−0.0832
0.5	1.1	0.2	7	0.5	0.78	2	0.5	8.4804	0.0344	−0.3638	−4.2929	−0.3094	−0.0958
						3		8.3277	0.0149	−0.3397	−4.1575	−0.2671	−0.1067
							0.5	8.3452	0.0177	−0.3502	−4.1584	−0.2923	−0.1096
0.5	1.1	0.2	7	0.5	0.78	1.2	1	8.4963	0.0767	−0.3724	−4.2946	−0.3291	−0.0981
							0.5	8.6666	0.1423	−0.3967	−4.4495	−0.3721	−0.0849

The Table 1 represents the variations in the drag force on vessel walls, Nusselt and Sherwood numbers for various parameters $(M, \lambda, \phi, Pr, Sr, Sc, Rd, S)$. Significant variations are observed as assumed in the mathematical structure. Increasing intensity of the magnetic field parameter $M(0.5, 1, 1.5)$ decreases the skin friction (C_f) on the walls, where the volume fraction $\phi(0.02, 0.1, 0.2)$ increases the skin friction (C_f) on the walls for the constant values of the different parameters mentioned in Table 1, while simultaneously, other transfer rates are unchanged. Increasing values of the Prandtl number Pr, Soret parameter Sr, Schmidt number Sc, Radiation parameter Rd, and the heat source parameter S affects all three coefficients skin fraction C_f, Nusselt N_u, and Sherwood number Sh. Very slight changes are seen in the heat transfer rate and mass transfer rate. This indicates a slow loss of body mass and temperature reduction.

5. Conclusion

The present study is carried out to examine the blood transport variations along with drug suspensions under the effect of volume fraction, chemical reaction, heat, and mass transfer on two-phase flow behavior in tumor surrounding regions, which are found at the bifurcation of arteries. Effects of various parameters on flow profiles of blood-carrying suspensions (drug), temperature fields, and concentration profiles that play a significant impact on various therapies are concluded as follows:

- The flowing two-phase fluid (blood) and suspension (drug particles) mixed with are transported with varying velocity profiles and pulsating nature. The walls have very low-profile velocities compared to the central region of the flow.
- The drug-carrying fluid supports the transport of the drug in the affected region as the suspension velocity is less compared to the drug carrier. Some parts of the drugs are absorbed by the pores of the flow region at that moment flow increases rapidly. Thus, the suspension is pushed by the fluid career.
- The increasing magnetized region (M) that is applied at different increasing angles (α), G(suspension mass parameter), decay parameter(λ), R (particle concentration parameter), Prandtl number (Pr), Chemical reaction parameter (ϑ) and radiation parameter (Rd) gives a reduced flow as the high concentration is used within the flow channel to treat the affected region. In the presence of dense suspensions (heavy drug load), low diffusions and reduced flow rates give good indications to reduce inflammations.
- Rising values of K (porosity parameter), β'(volumetric expansion parameter for concentration), ϕ (volume fraction parameter, and heat source (S) increases the velocity for both the fluid phases. These increasing velocities need to be monitored during treatment, as high flow rates will lead to a jump in pressure on the walls of the fluid carrier.
- Increasing λ, Schmidt number (Sc), Soret number (Sr), Chemical reaction parameter (ϑ)and heat source parameter (S) reduces the concentration profile of the affected area as diffusion is reduced.
- Rising values of Prandtl number (Pr) increases the concentration profile.
- Thermal profiles are reduced for increasing radiation (Rd) and Prandtl number (Pr), where the heat source (S) is increasing thermal profiles.
- In the drug delivery systems, homogeneous chemical reactions of first order are taking place that enhance the efficacy of the system. This is measured as the effect of the chemical reaction parameter (ϑ).

- The Soret number (Sr) witnessed in Table 1 shows a significant reduction in wall stresses, and the mass transfer rate is drastically high, indicating the high efficacy of the drug delivery systems. This application will be helpful in tumor treatments.
- Volume fraction (ϕ) need to control as by absorption of drugs, walls are stressed more listed in Table 1. Most of the interventions (various parameters) affect the skin fraction C_f on walls, and slightly changing heat flow from the object and mass reduction is also slow. This can be used as a clinical observation of tumor treatments.

The above results are based on a mathematical formulation and computational approach. Further, these numerical approaches need to be validated clinically under the supervision of medical experts.

Acknowledgements

This research project was funded by the University of Technology and Applied Sciences, Shinas, through the Internal Research Funding Program-2024, grant number (UTAS-Shinas-cy01-2024-005).

The authors acknowledge valuable suggestions from the reviewers and the editorial board members that enhance the quality of the manuscript.

References

[1] World health organization news 01-02-2024. https://www.who.int/news/item/01-02-2024-global-cancer-burden-growing–amidst-mounting-need-for-services.

[2] L T Baxter and R K Jain. Transport of fluid and macromolecules in tumors: I. role of interstitial pressure and convection. *Microvascular research*, 37(1):77–104, 1989.

[3] L T Baxter and R K Jain. Transport of fluid and macromolecules in tumors: Ii. role of heterogeneous perfusion and lymphatics. *Microvascular research*, 40(2):246–263, 1990.

[4] L T Baxter and R K Jain. Transport of fluid and macromolecules in tumors: Iii. role of binding and metabolism. *Microvascular research*, 41(1):5–23, 1991.

[5] R K Jain. Transport phenomena in tumors. In *Advances in chemical engineering*, volume 19, pages 129–200. Elsevier, 1994.

[6] N P Singh and A K Singh. Mhd effects on heat and mass transfer in flow of a dusty viscous fluid with volume fraction. *Indian Journal of Pure and Applied Physics*, 39:496–509, 2001.

[7] H M Byrne and J R King. A two-phase model of solid tumour growth. *Applied Mathematics Letters*, 16(4):567–573, 2003.

[8] I I Bogdanov, V V Mourzenko, J F Thovert, and P M Adler. Two-phase flow through fractured porous media. *Physical Review E*, 68(2):026703, 2003.

[9] O Prakash, S P Singh, D Kumar, and Y K Dwivedi. A study of effects of heat source on mhd blood flow through bifurcated arteries. *AIP advances*, 1(4), 2011.

[10] A Chaudhuri, C F Osterhoudt, and D N Sinha. Determination of volume fractions in a two-phase flows from sound speed measurement. In *Noise Control and Acoustics Division Conference*, volume 45325, pages 559–567. American Society of Mechanical Engineers, 2012.

[11] Z Abbas, J Hasnain, and M Sajid. Mhd two-phase fluid flow and heat transfer with partial slip in an inclined channel. *Thermal Science*, 20(5):1435–1446, 2016.

[12] K R Madhura and D S Swetha. Influence of volume fraction of dust particles on dusty fluid flow through porous rectangular channel. *International Journal of Mathematics Trends and Technology-IJMTT*, 50, 2017.

[13] I M Eldesoky. Mathematical analysis of unsteady mhd blood flow through parallel plate channel with heat source. *World Journal of Mechanics*, 2(3):131–137, 2012.

[14] H Chen, X Tong, L Lang, O Jacobson, B C Yung, X Yang, R Bai, D O Kiesewetter, Y Ma, H Wu, G Niu, and X chen. Quantification of tumor vascular permeability and blood volume by positron emission tomography. *Theranostics*, 7(9):2363–2376, 2017.

[15] R K Thulborn, A Lu, I C Atkinson, M Pauliah, K Beal, T A Chan, A Omuro, J Yamada, and M S Bradbury. Residual tumor volume, cell volume fraction, and tumor cell kill during fractionated chemoradiation therapy of human glioblastoma using quantitative sodium mr imaging. *Clinical Cancer Research*, 25(4):1226–1232, 2019.

[16] H F Vazifehshenas and F Bahadori. Investigation of soret effect on drug delivery in a tumor without necrotic core. *Journal of the Taiwan Institute of Chemical Engineers*, 102:17–24, 2019.

[17] B Wirthl, J Kremheller, B A Schrefler, and W A Wall. Extension of a multiphase tumour growth model to study nanoparticle delivery to solid tumours. *PLoS One*, 15(2):e0228443, 2020.

[18] A Bera, S Dutta, J C Misra, and G C Shit. Computational modeling of the effect of blood flow and dual phase lag on tissue temperature during tumor treatment by magnetic hyperthermia. *Mathematics and Computers in Simulation*, 188:389–403, 2021.

[19] E Omamoke, E Amos, and E Jatari. Impact of thermal radiation and heat source on mhd blood flow with an inclined magnetic field in treating tumor and low blood pressure. *Asian Research Journal of Mathematics*, 16(9):77–87, 2020.

[20] D Kumar, S Bora, R Kumar, S Kumar, and N Deo. Application of heat source and chemical reaction in mhd blood flow through permeable bifurcated arteries with inclined magnetic field in tumor treatments. *Results in Applied Mathematics*, 10:100151, 2021.

[21] G Liu, L Yang, G Chen, F Xu, F Yang, H Yu, L Li, X Dong, J Han, C Cao, J Qi, J Su, X Xu, X Li, and B Li. A review on drug delivery system for tumor therapy. *Frontiers in pharmacology*, 12:735446, 2021.

[22] V Darvishi, M Navidbakhsh, and S Amanpour. Heat and mass transfer in the hyperthermia cancer treatment by magnetic nanoparticles. *Heat and Mass Transfer*, 58(6):1029–1039, 2022.

[23] H Wang, A Alizadeh, A M Abed, A Piranfar, G F Smaisim, S K Hadrawi, H Zekri,

D Toghraie, and M Hekmatifar. Investigation of the effects of porosity and volume fraction on the atomic behavior of cancer cells and microvascular cells of 3dn5 and 5otf macromolecular structures during hematogenous metastasis using the molecular dynamics method. *Computers in Biology and Medicine*, 158:106832, 2023.

[24] N A Shah, B Almutairi, D Vieru, B Lee, and J D Chung. Bioheat transfer with thermal memory and moving thermal shocks. *Fractal and Fractional*, 7(8):629, 2023.

[25] B Shakya. The role of chemistry in cancer chemotherapy: A mini review. *Amrit Journal*, 3(1):49–56, 2023.

[26] N Yadav, S Jaiswal, and P K Yadav. Two-phase magnetohydrodynamic blood flow through curved porous artery. *Physics of Fluids*, 36(9), 2024.

[27] A Girema, Y Y Gambo, and B Y Haruna. Unsteady mhd blood flow through bifurcated arteries with heat source and magnetic field in the presence of soret effect. *International Journal of Scientific Research in Mathematical and Statistical Sciences*, 11:66–74, 12 2024.

[28] M Zamir and M R Roach. Blood flow downstream of a two-dimensional bifurcation. *Journal of theoretical biology*, 42(1):33–48, 1973.